Enhancement of System Observability During System-Level Radiation Testing Through Total Current Consumption Monitoring

Ivan Slipukhin, Andrea Coronetti, *Associate Member, IEEE*, Rubén García Alía, *Member, IEEE*, Frédéric Saigné, Jérôme Boch, Luigi Dilillo, *Member, IEEE*, Ygor Q. Aguiar, *Member, IEEE*, Carlo Cazzaniga, Maria Kastriotou, and Torran Dodd

***Abstract*— System-level testing of electronics is an affordable method of assessment of the performance of complete electronic systems designed for applications in the radiation environment. Compared to component-level testing, system-level test offers a much smaller degree of observability about the performance of particular system elements. The information received during the irradiation of a system might be therefore not sufficient for the identification of every system under test (SUT) malfunction. As a consequence, no action might be taken to recover the system operation while certain parts of its functionality would be lost due to the radiation-induced effects. This can lead to the incorrect execution of the system-level test and improper conclusions about radiation-induced effects. The present paper demonstrates a method allowing an efficient identification of system-level failures based on the system total current consumption monitoring. The proposed technique can be easily implemented with common instrumentation and at the same time provides valuable feedback on SUT operation. The retrieved current consumption information can be used to identify system failures that may be not observable through the communication channels that are by default included in the tested setup. Furthermore, the posttest analysis can be performed on the collected data to investigate the SUT condition along the complete timeline of its irradiation. The verification of the proposed method was performed during the qualification test of a system designed for applications at the high-energy particle accelerator facility.**

***Index Terms*— CERN high-energy accelerator mixed-field (CHARM) facility, ChipIr, radiation hardness assurance (RHA), singe-event effect (SEE), system observability, system-level test.**

Manuscript received 8 April 2024; revised 14 June 2024; accepted 2 July 2024. Date of publication 5 July 2024; date of current version 16 August 2024. This work was supported by European Union's Horizon 2020 Research and Innovation Program under Grant 101008126. *(Corresponding author: Ivan Slipukhin.)*

Ivan Slipukhin and Andrea Coronetti are with CERN, 1211 Geneva, Switzerland, and also with the Institute d'Électronique et des Systémes, Université de Montpellier, 34090 Montpellier, France (e-mail: ivan.slipukhin@cern.ch).

Rubén García Alía and Ygor Q. Aguiar are with CERN, 1211 Geneva, Switzerland.

Frédéric Saigné and Jérôme Boch are with the Institute d'Électronique et des Systémes, Université de Montpellier, 34090 Montpellier, France.

Luigi Dilillo is with the Institute d'Électronique et des Systémes, Université de Montpellier, CNRS, 34090 Montpellier, France.

Carlo Cazzaniga, Maria Kastriotou, and Torran Dodd are with the ISIS Facility, U.K. Research Innovation (UKRI)-Science and Technology Facilities Council (STFC), SN2 1SZ Swindon, U.K.

Color versions of one or more figures in this article are available at https://doi.org/10.1109/TNS.2024.3424201.

Digital Object Identifier 10.1109/TNS.2024.3424201

I. Introduction

THE performance of the finalized electronic system can be inferred from the component-level test results through data analysis or simulations [1]. The precision of such analysis might be compromised because of the simplification of the utilized circuitry, component variability, and integrated circuits' (ICs) operating conditions different compared to the component-level test. System-level testing in the radiation field that will be encountered at the systems' destination environment, in combination with component-level test data, gives a more realistic estimate of possible radiation-induced effects and degradation. Such analysis of system performance is advised for the design of highly critical electronics for accelerators [2].

The primary objective of the work is the enhancement of radiation hardness assurance (RHA) procedures designed for the CERN accelerator complex, where the environment is often accompanied by the radiation field arising as a consequence of accelerator operation [3]. A dedicated approach to system design and testing at CERN has been proven to have a positive influence on the radiation tolerance of electronics [4]. As a means of evaluation of the proposed methodology, this article demonstrates the result of a test campaign targeting an important aspect of electronic systems' operation in the accelerator radiation field: radiation-induced single-event effects (SEEs). The reported system-level test consisted of system irradiation with an atmospheric neutron beam provided by the ChipIr facility [5]. It creates the high-energy hadron (HEH) field, resembling the one in the proximity of accelerators, and which accounts for the majority of the SEE-induced failures in accelerator electronics.

One of the main issues of system-level radiation testing is that the identification of the criticality of the failures is often complicated by the fact of dealing with a complex system, where different effects may result in an identical observation. The enhancement of system observability can provide an additional source of information for a more efficient identification of the failures encountered during the system irradiation. The improvement of system observability has been previously demonstrated by the implementation of software-based instrumentation cores in a system-on-a-chip (SoC) [6],

© 2024 The Authors. This work is licensed under a Creative Commons Attribution 4.0 License.
For more information, see https://creativecommons.org/licenses/by/4.0/

where the performed observations also provided sufficient data to identify the failure root causes. However, system-level testing, involving both analog and digital circuitry implemented externally to an SoC, requires a different approach; the observation technique should collect the data representing the operation of multiple ICs used in the design. Another example of system under test (SUT) observations was implemented during system-level irradiation of an SoC-based module [7], but utilized the SUT internal circuitry to perform the system observations. The disadvantage of such an approach is that the measurement device is also subjected to the effects of the radiation field, which may result in erroneous data readout or loss of measurement. The complete system design familiarity substantially simplifies testing and diagnostics [8], however, it is hard to generalize the methodology implemented during such system-level tests to every SUT case, especially to those with limited knowledge of the design. An efficient method has been proposed [9] by performing continuous monitoring of analog signals located at different sensitive nodes of the SUT. This approach has shown the possibility to detect single-event transients (SETs) responsible for system failures. In another study [10], the sampling of a set of signals around the SUT allowed to determine the components with the highest total ionizing dose (TID) degradation, used in the system. Sampling of SUT total current consumption has been previously used as a part of system monitoring during irradiation [11], which is also the case in two aforementioned studies, however, was not utilized by itself for the purposes of SUT failure mode (FM) identification during irradiation.

In this article, we demonstrate the possibility of improving the observability for digital and mixed-signal systems through the means of periodic sampling of the SUT total current. The detailed analysis of the current consumption can then be used to determine the criticalities of the SUT failures during the system-level test, and to classify the observed FMs. The proposed methodology is based on the monitoring of the overall current consumption of the SUT in time and its correlation with observations made through data retrieved from the SUT. A set of software-level observations has been implemented for the purposes of a more complete monitoring of the radiation-induced effects during the methodology evaluation. The total current consumption monitoring is a common practice during system-level testing [12], [13] and is often implemented as one of the default SUT observations, however, the analysis of the recorded data is usually limited to single-event latch-up (SEL) detection and the qualitative study of these effects [14], [15]. The instantaneous value of the current consumption is then compared with the threshold current to make a binary decision about the presence of an SEL. This approach can be possibly improved by observing multiple conditions in the SUT current consumption, which can lead to the detection of a wider range of SEEs on the system level.

In this article, Section II describes the proposed system observation approach, Section III gives the description of the experiment executed to test the proposed method, Section IV focuses on the analysis of the test results and the performance of the methodology, Section V includes the discussion of benefits and limitations of the proposed approach, and finally, in Section VI, the conclusions about the accomplished work are given.

II. Proposed System Observation Approach

The proposed system observation approach implies the inclusion of the following elements during system-level testing.

1) SUT total current consumption sampling with a periodicity of around 1 s. For the methodology verification, this was accomplished by measurement of the current drawn at the output of the power supply module (the SUT required a single +12 V voltage line). This is a simple implementation of such monitoring that can be usually performed with the embedded functionality of the power supply and does not require dedicated instrumentation.
2) The implementation of software-level observations of the SUT. These measurements require only the default communication link with the SUT and are performed with an additional data transfer through it. In the system-level test described in this article, they served as a main source of the SUT diagnostics during irradiation (based solely on these observations, the conclusions were made during the test about the SUT state). In particular, the test setup was retrieving the data being a part of the normal functionality of the system, as well as additional information was gathered from the system to increase the observability of its operation during the test. These measurements included system real-time clock (RTC) value and board temperature. Similarly, the sampling of these data was logged by the host PC once per second.
3) Correlation of observations made through the total current consumption monitoring with the software-level observations in the posttest data analysis using a common timeline. This allows to establish the correspondence between both types of observations and to incorporate the current consumption observation in the system FM analysis.

Furthermore, as it will be shown, the observation of the total current consumption can be used during irradiation as an additional source of information to determine the SUT state, i.e., the identification of normal and failed operation.

III. Experiment Overview

A. System Under Test

The proposed method for system-level observation was verified using a custom-built electronic system. The chosen SUT is a general-purpose single-event effect (SEE) tester that was designed to qualify digital and analog ICs at the CERN high-energy accelerator mixed field (CHARM) irradiation facility [16]. The system contains all the necessary functionality to configure and test the device under test (DUT) with the possibility to detect SEEs by means of digital and analog communication. Moreover, the tester includes the necessary circuitry for the detection of SELs with subsequent restoration of the DUT functionality. The whole system required a single +12 V power supply line to provide power to all its elements, including the DUT.

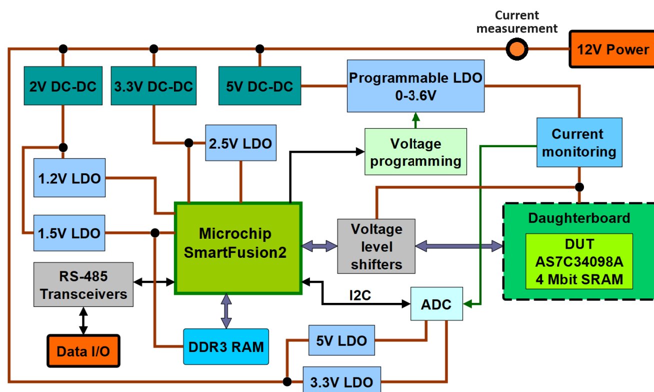

Fig. 1. Block diagram of the SUT. The total current consumption monitoring was performed on the line labeled "12 V Power."

The SUT was designed following a radiation-tolerant approach to sustain the irradiation during a single-week CHARM test in the harshest position, designated as R13. The CHARM facility recreates the radiation field that can be found nearby high-energy particle accelerators. It is mainly composed of HEHs, such as protons, pions, and neutrons with a broad spectrum, spreading from thermal energies up to several GeV. This radiation field is also accompanied by spectra of photons and electrons that contribute to TID. In such an environment, the SUT is concurrently subjected to both TID and displacement damage (DD) degradation, as well as SEEs. While being subjected to the mixed radiation field of position R13, the tested system should comply with the following requirements.

1) Retaining its functionality up to the total dose of 500 Gy.
2) Having the mean time between failures (MTBFs) of at least 6 h.

Taking into account the HEH fluence at the position R13, it corresponds to the maximum SEE-induced failure cross section of $3.15{\cdot}10^{-11}$ cm^2/system. The radiation tolerance of the system will allow performing the correct SEE testing of ICs with a low level of disturbance originating from the susceptibility to radiation effects of the tester itself.

The design of the tester system is based on the commercial off-the-shelf components (COTS) previously characterized at the component level for other CERN uses. The majority of them have been tested with the HEH radiation field and demonstrated a sufficient degree of radiation tolerance for the targeted operating conditions. The system consists of the motherboard with Microchip SmartFusion2 SoC as the main processing unit, and a customizable daughterboard hosting the IC under test (Fig. 1). The SmartFusion2 SoC has been previously proven to be tolerant to TID up to 650 Gy, and to have low SEU cross section of the register logic in the field programmable gate array (FPGA) subsystem [17]. The implementation of the gateware design in the SmartFusion2 SoC was done utilizing the register-level triple modular redundancy (TMR) technique.

For the purposes of the system-level test, the SUT was configured to perform a functionality typical for its normal operation. The daughterboard was hosting a static random access memory (SRAM) manufactured by Alliance. This memory was the DUT and the system was performing its continuous monitoring to detect single event upsets (SEUs) and SELs that might have occurred in the SRAM while it was irradiated.

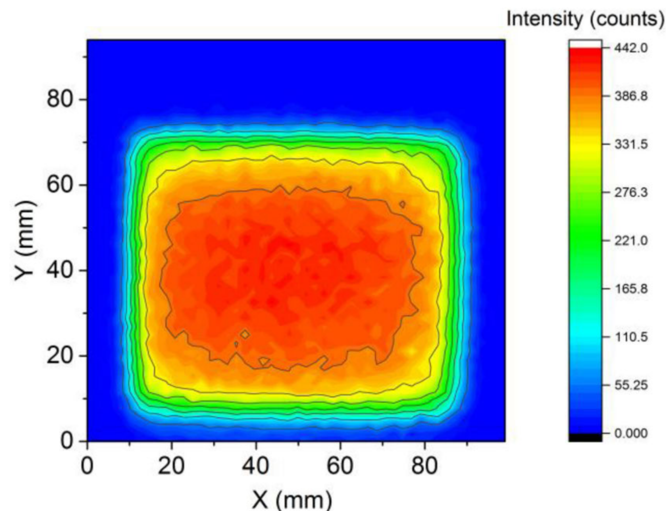

Fig. 2. Measurement of the relative intensity of the neutron beam with the area of 70×70 cm^2 provided by the ChipIr facility [5]. The dimensions of the beam were adjusted to the size of the SUT.

B. Test Configuration and Objectives

The aim of the performed test was to investigate the SEE-induced system failures under a radiation field representing the HEH (above 20 MeV) component of the radiation field of the CHARM facility. The atmospheric neutron beam with a spectrum ranging from thermal neutrons to high-energy (up to 800 MeV) was provided by the ChipIr instrument, which is a part of the ISIS facility (based at the Rutherford Appleton Laboratory, Didcot, U.K.). During irradiation, the neutron flux was measured by monitoring the high-energy part of the spectrum and was on average equal to $5.6 \cdot 10^6$ n/cm^2/s. The neutron beam is characterized by the high homogeneity over a large area (Fig. 2) which allows for accurate testing of large systems.

The test consisted of simultaneous irradiation of four stacked SUTs (Fig. 3). Therefore, three out of four systems were subjected to the neutron beam that has already passed through the volume of other printed circuit boards (PCBs) placed closer to the beam guide output. Due to the fact that neutrons, unlike charged particle species, do not lose their energy through direct matter ionization, the loss of beam intensity was negligible. The utilization of a neutron beam simplifies the testing of complete systems, in which complex geometry is normally a source of energy attenuation when a charged particle beam is used [18]. For the same reason, the utilization of atmospheric neutron beam allows excluding any TID degradation of the tested system and isolating the system-level test to only SEE-induced failures. The beam profile was adjusted to cover the entire area of the SUT and DUT, and had a rectangular shape with sides of 11 and 19 cm, respectively. The beam profile has been aligned with the geometrical center of the SUT.

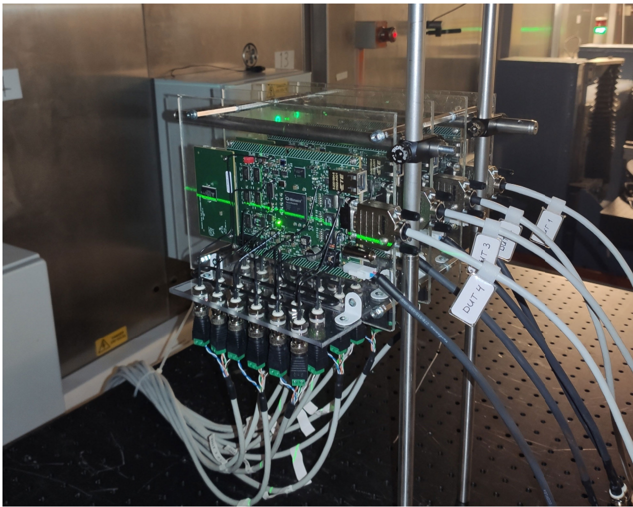

Fig. 3. Stack of four Systems Under Test installed at the ChipIr facility in front of the neutron beam guide output.

The set of software observations concerned the data retrieval from the SUT using the default digital interface (RS-485). The data that were normally collected from the SUT were related to the DUT observations, i.e., SEU and SEL monitoring of an SRAM IC. Moreover, apart from the parameters mentioned in the Section II, the software observations included the voltage and current consumption monitoring of the DUT. The total current consumption of each of the SUTs was recorded with the 100 μA precision.

IV. System-Level Testing Results and Analysis

A. System-Level Test Summary

The results presented below are the outcome of the observations gathered during 54 h of continuous irradiation of four SUTs under the atmospheric neutron beam. The total high-energy neutron fluence (energies above 10 MeV) collected over this time period was equal to $1.11 \cdot 10^{12}$ n/cm^2. All of the tested SUTs remained functional until the end of the irradiation. Furthermore, no degradation in the system's performance has been observed, i.e., the frequency of system failures was not increasing over the irradiation time.

System failures were initially detected solely based on the set of software observations; the current consumption monitoring was executed in parallel throughout the whole duration of the test, but was not taken into account for the failure detection during irradiation and was only used in posttest analysis. The SUT FMs were identified during the test and assigned to different criticality classes depending on their severity. The amounts of failures initially attributed to each FM are reported in Table I. The classification of FMs by criticality classes is based on the one proposed in another study of system-level testing methodology [19] and is presented in Table II. For each criticality class, the initial system-level failure cross sections were calculated.

A predefined decision logic, based on the software observations, was applied during the test by the operator to perform the system recovery after the functionality was lost. For each criticality class, a specific action was executed immediately after the failure encounter, which was either SUT reconfiguration, SUT power cycle, or no intervention. All recorded failures were either transparent to the system (not visibly affecting it in any way) or led to a soft or hard loss of functionality.

TABLE I
Counts of FMs for Each SUT According to Initial Classification

	Failure mode									
SUT	0	1	2	3	4	5	6	7	8	**Total**
1	1	74	2	5	29	25	3	33	3	175
2	4	82	3	5	38	31	6	29	4	202
3	3	77	0	3	41	28	2	26	5	182
4	8	71	3	2	37	28	1	37	8	187

TABLE II
Observed SEE-Induced FMs of the Systems Under Test

Criticality class	**FM**	**Color code on Figures**	**Description**	**Action**
Transparent to the system	T0	Dotted black	Error in data received from SUT	No action
	T1	Dotted green	Local time reset to the default value (2000-01-01 00:00:00)	
	T2	Dotted blue	Local time reset to non-default value	
	T3	Dotted yellow	Board temperature wrong reading	
Soft loss of functionality	S4	Dashed red	Loss of communication, with subsequent reconfiguration and restart	SUT reconfiguration
Hard loss of functionality	H5	Dashdot brown	Loss of communication and failure to retrieve software observations	SUT power cycle
	H6	Dashdot grey	Loss of communication and failure to retrieve system state information	
	H7	Dashdot violet	Non-recoverable communication loss	
	H8	Dashdot orange	Error related to SEL monitoring system	
Permanent loss of functionality	-	-	(Not observed)	SUT power down

B. Posttest Analysis of Collected Data

In the posttest analysis, all system failures observed during irradiation were correlated to the recorded current supplied to each of the SUTs. In Figs. 4–7, the regions with a blue background highlight the time over which the SUT was correctly performing the monitoring of the SRAM. This information was used to confirm the partial loss of functionality of the SUT. Pink solid lines are the timestamps of the SELs detected by the tested system in the DUT. Other events mentioned in the figures are the FM4, labeled with the red dashed line and FM1, labeled as a green dotted line.

The lack of active monitoring of the SRAM by the SEE tester system can be normally linked to system FMs detected through software observations. These failures, in turn, can be

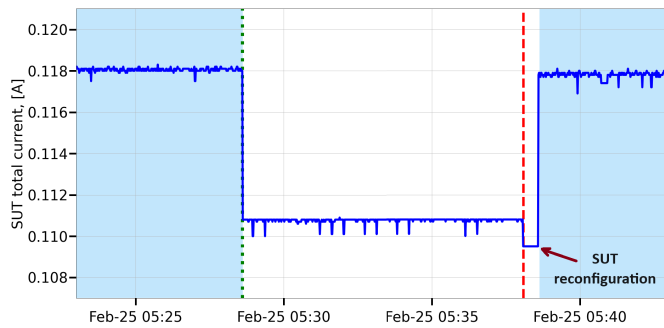

Fig. 4. Blue background—SUT performing the monitoring of the SRAM. This fragment of the current consumption observation demonstrates the correlation of SUT2 loss of functionality with the occurrence of FM 1 and a decrease in the consumed current. Since this FM 1 was not initially considered as a loss of functionality, no action was taken to restore the system operation until the occurrence of the FM 4.

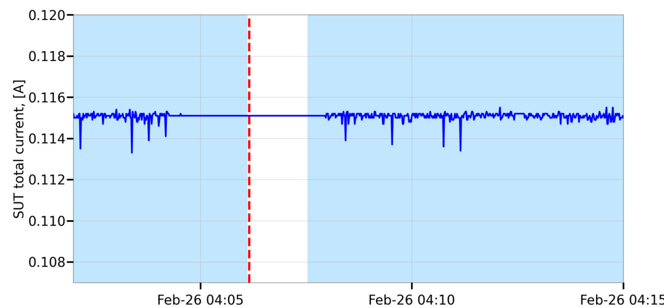

Fig. 5. Blue background—SUT performing the monitoring of the SRAM. In the shown situation, a soft loss of SUT3 functionality (FM 4) is not accompanied by the total current consumption decrease (the only observed case among four SUTs).

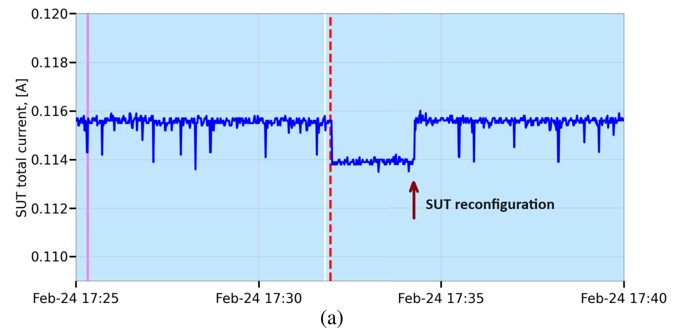

(a)

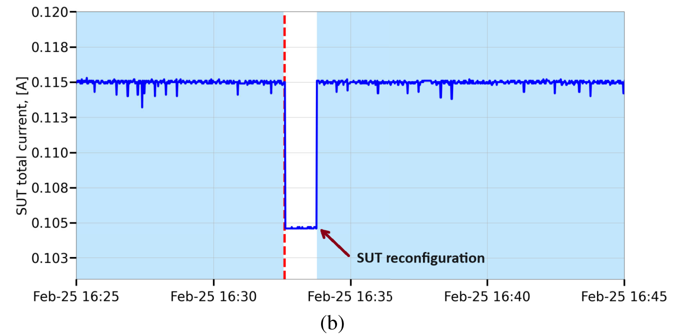

(b)

Fig. 6. Blue background—SUT performing the monitoring of the SRAM. In the given examples, soft losses of SUT4 functionality (FM 4), can be associated with different changes in SUT total current consumption. FM 4 followed by the current consumption decrease of around (a) 1 mA and (b) 8 mA.

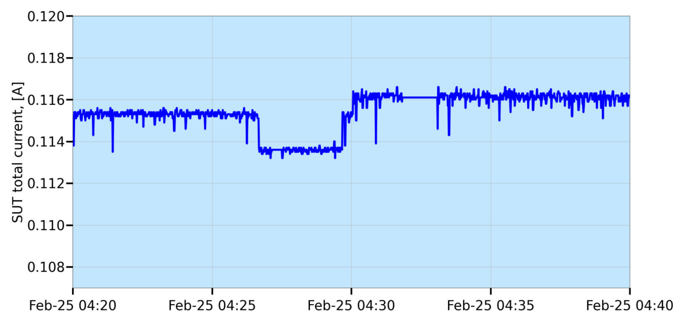

Fig. 7. Blue background—SUT performing the monitoring of the SRAM. In the given time period, the reduction of SUT3 current consumption is not correlated with any event recorded with the software observations.

associated with the features of the current consumption evolution. For example, every loss of functionality is accompanied by a certain recorded event beforehand and in most cases can be also correlated with a drop in current consumption.

It should be noted that most of the failures classified as soft and hard losses of functionality are accompanied by the reduction of current consumption. In particular, every soft loss of functionality can be associated with an abrupt decrease of the current consumed by the SUT (Fig. 4), provided that the system was in a fully functional state before it (the only exception was observed in SUT3, on February 26 around 4:00, Fig. 5). Decreases of current consumption were also noted before the events that were assumed to be transparent to the system functionality (assigned to FMs 1 and 2). At the same time, the postanalysis of the collected data has revealed that the SUT was stopping to perform the DUT monitoring during the periods of decreased current consumption. This was observed by the absence of recordings of the SEU or SEL event data from the DUT, despite the presence of impinging neutron beam. During the test campaign, this behavior was not noted and thus no action was taken to restore the system operation on the occurrence of such events, the SUTs were kept running until a more severe failure was encountered that required system reconfiguration or power cycle. Hence, if the current consumption information was taken into account during the system-level test, FMs 1 and 2 would have been classified as soft or hard losses of functionality, depending on how the SUT could be recovered after their occurrence. A posteriori, the cross sections can be reassessed considering these FMs as soft losses of functionality. As a consequence, a significant increase in the failure cross section of this criticality class can be observed. Table III demonstrates the influence of the current consumption observation on the total cross section of different FMs grouped by the criticality classes.

Apart from criticality class reassignment, the performed observation brings the necessity to reduce the total received fluence of the SUTs. The time through which systems were not functional due to incorrect FM identification, cannot be counted as an effective system-level test time, thus the received fluence cannot contribute to the failure cross-section calculation. This was taken into account for the calculation of the updated failure cross sections reported in Table III. While the cross section of events that are transparent to the system does not deviate significantly, the cross section of soft losses of functionality has increased on average by the factor of 2.75.

TABLE III

TOTAL FAILURE CROSS SECTION BEFORE AND AFTER THE INCLUSION OF CURRENT CONSUMPTION OBSERVATION

Criticality		Failure cross-section, [cm²/system]			
		SUT1	SUT2	SUT3	SUT4
Transp. to the system	Before	$7.40 \cdot 10^{-11}$	$8.48 \cdot 10^{-11}$	$7.49 \cdot 10^{-11}$	$7.58 \cdot 10^{-11}$
	After	$7.76 \cdot 10^{-11}$	$1.02 \cdot 10^{-10}$	$7.17 \cdot 10^{-11}$	$8.28 \cdot 10^{-11}$
Soft loss of functionality	Before	$8.39 \cdot 10^{-11}$	$9.74 \cdot 10^{-11}$	$9.20 \cdot 10^{-11}$	$1.00 \cdot 10^{-10}$
	After	$2.29 \cdot 10^{-10}$	$2.89 \cdot 10^{-10}$	$2.56 \cdot 10^{-10}$	$2.53 \cdot 10^{-10}$

In the case of events classified as soft losses of functionality, although grouped as a single FM based on the software-recorded data, two separate types can be distinguished based on the changes in current consumption (Fig. 6). For each SUT, the decreases in current consumption were either by around 1 mA [Fig. 6(a)] or 8 mA [Fig. 6(b)], and in both cases, the functionality of the SUT could be restored by system reconfiguration. In the case of a smaller current decrease, the tested system was still capable of performing the DUT monitoring. Although such behavior is not significant as far as the criticality class is concerned, these events might reveal a partial loss of the system functionality, that is either not actively involved in its operation or is not properly covered by the implemented software observations. The capability of DUT monitoring signifies the continuity in the FPGA operation of the SoC, therefore, the loss of functionality in this case can be associated with the failure of the microcontroller, or another part of the SoC. In the analysis of SEE-induced failures, two types of FMs can be therefore distinguished.

Certain events that were observed in the evolution of the current consumption cannot be correlated with the events seen through the software observations. For example, the recorded waveforms contain features that can be characterized by a sudden decrease of supply current by around 1 mA, with a subsequent return to the previous current value after several minutes of operation (Fig. 7). Such variations of current consumption cannot be caused by the normal functionality of the SUTs since no changes to their configuration were applied, and the tested systems cannot independently enter a different mode of operation, impacting the drawn current. Considering the constant exposure of the SUTs to the neutron beam, these events can be the signatures of radiation-induced SEEs affecting the parts of the system not directly involved in the performed functionality. Such events would be transparent to the system operation and not result in any changes in data collected with software. The implementation of additional system observations might allow to identify the FMs associated with such events.

Based on the performed analysis of the SUT current consumption profiles, an updated classification of FMs and their criticality classes can be constructed (Table IV). In accordance with the assumption made for failure cross-section calculation, FMs 1 and 2 will be moved to the soft loss of functionality class. Furthermore, in the same criticality class, the observed cases of FPGA functionality retention require a split of FM 4 into two types of failures, now numbered as 4 and 10. The FM 10 accounts for the situation in which the failure was likely associated with just the microcontroller part of the system.

TABLE IV

OBSERVED SEE-INDUCED FMs OF THE SYSTEMS UNDER TEST WITH CORRECTIONS BASED ON THE CURRENT CONSUMPTION OBSERVATION

Criticality class	FM	Description
Transparent to the system	T0	Error in data received from SUT
		Local time reset to the default value (2000-01-01 00:00:00)
		Local time reset to non-default value
	T3	Board temperature wrong reading
	T9	Undetected failure associated with the abrupt change in current consumption
Soft loss of functionality	S4	Loss of communication, with subsequent reconfiguration and restart
	S10	Loss of communication, with subsequent reconfiguration and restart, retention of DUT monitoring
	S1	Local time reset to the default value (2000-01-01 00:00:00)
	S2	Local time reset to a non-default value
Hard loss of functionality	H5	Loss of communication and failure to retrieve software observations
	H6	Loss of communication and failure to retrieve system state information
	H7	Non-recoverable communication loss
	H8	Error related to SEL monitoring system
Permanent loss of functionality	-	(Not observed)

The sudden changes in the current consumption of the SUTs are likely signatures of the SEEs occurring in the system, as those cannot be a consequence of change in the system functionality, which has remained unchanged during irradiation. The possible data retrieval from the DUT cannot be a likely cause of the change in the current consumption evolution since it can be only associated with the temporal increase in current consumption, which was not observed. Based on this observation, a new FM can be distinguished and classified as transparent to the system functionality, since no related observation was made on the software level.

V. DISCUSSION OF THE PROPOSED METHODOLOGY

The proposed approach provides a substantial contribution to the system observation data used in the posttest analysis. At the same time, its implementation does not require any modification of the SUT and can be adapted for any specific application and complexity of the tested system.

The monitoring of the SRAM, implemented in the SUT, provided valuable data for the analysis of the system availability. The tested Alliance SRAM is characterized by

high SEL [20] and SEU [21] cross sections in the neutron field. The frequency of occurring SEEs during irradiation at ChipIr was high enough (at least 1 event/s) to use the readouts of the occurring SEEs as an indication of the presence of the full system functionality. In the posttest data analysis, this observation helped to exclude the irradiation time spent during the power-on sequence and SUT configuration for the calculation of the final failure cross sections. This approach is specific to the tested system and cannot be replicated or used as a part of the methodology for every SUT case. Depending on the architecture of the system, such measurement can be replaced with the monitoring of certain reoccurring events in the system, such as local clock update, Watchdog timer reset, or other periodic system interrupts.

The sampling rate of around 1 sample/s in both current consumption monitoring and the execution of software observations appears sufficient for the methodology implementation and can be potentially further decreased. Detection of a particular mode of operation of the system was based on the collection of multiple current consumption samples of comparable values not exceeding the inherent noise amplitude (~300 μA for the studied case). The observation of the transition to another stable value of current consumption was the only event considered to be significant for the system-level failure analysis in this study. Depending on the tested system, the sampling speed might need to be increased so that faster transitions between different modes of operation can be captured. The SUT can be often characterized by short-lasting, occasional shifts to other modes of operation. In the case of the tested system, such temporal states can be associated, for example, with the transitions to the SRAM rewrite operations. These changes are stochastic and cause an increase in the current consumption with a short duration (hundreds of nanoseconds). If the test instrumentation does not allow to resolve such fast changes in current consumption (i.e., by collecting several samples to detect a stable value), the sampling speed should be reduced so that the associated changes of current consumption are averaged, which was implemented in the described test setup.

Certain radiation-induced effects can be transparent to the system and not result in system-level failures; this does not preclude their observation in the current consumption evolution, where they can possibly postulate themselves as short-lasting changes of its value. The selected sampling rate appears to be sufficiently low to exclude such events from the recorded data. Certain events, such as the one shown in Fig. 7, could be occasional exceptions. The described approach to system observation will mask the system-level effects that result in changes in current consumption that are too low to be detected, i.e., lower than the assumed current consumption thresholds.

A stable average current consumption of the tested system and its single mode of operation allowed for a clear distinguishment between normal and anomalous states of the SUT. Hence, the analysis of system-level failures based on the current consumption was in this case simplified compared to a more general case of an SUT which could enter multiple modes of operation, in which the supplied current can vary substantially [22], as well as system's susceptibility to different types of SEEs [23]. In a situation when an SUT transitions between different current consumption modes associated with different, yet normal modes of operation, the proposed approach for system monitoring would require additional considerations in the data analysis stage. The exact values of the SUT current consumptions in all modes of operation, including the power-on sequence, should be known beforehand, as well as the timestamps of transitions between them during the system-level test. Alternatively, a system can be tested in different modes of operation separately; the final analysis, including the failure cross-section calculation, will be conducted individually for each mode of operation [24]. If the decision logic is to be implemented for the duration of the test, the transition between different modes of operation should prevent the interpretation of the associated change in current consumption.

The required precision of the current consumption sampling is largely SUT-dependent since it will vary based on the used hardware elements and the software being executed at a particular time. It should be sufficiently high to distinguish between normal and faulty modes of operation, where the exact difference between associated current consumptions cannot be foreseen. The sampling resolution should be as high as possible and will be limited by the characteristics of the used instrumentation on one hand, and the noise introduced by the SUT on the other. The latter can be seen in Figs. 4–7 and is mostly associated with the operation of the SUT's switching power converters. For the tested system, the chosen resolution of 100 μA is sufficient and should remain below ~0.5 mA, based on the observed transitions in the drawn current (e.g., demonstrated in Figs. 6(a) and 7).

Current consumption monitoring can be used as a method to identify system malfunctioning, although by itself it has a very limited capacity to trace down the elements of the SUT responsible for the observed failures. The addition of supplementary observations, in both hardware (e.g., monitoring of sensitive voltages) and software can open a possibility for a detailed investigation of the observed failures and their root causes. As the system-level failures are often caused by fast SETs, an increase in the sampling rate will be also required. The selection of the exact current sampling speed will be a compromise between the volume of collected data, the occupancy of the data links, the precision of the time-stamping of system FMs, and effective SUT test duration.

VI. Conclusion

In this study, a new approach to SUT observation during system-level radiation testing was implemented and evaluated. The monitoring of SUT total current consumption provided additional data about the behavior of the SUTs during irradiation.

Data collected using the software observations during the system-level SEE testing allowed to determine a set of system-level FMs of the SUT. All observed FMs were assigned to different criticality classes. In the posttest data analysis, those were correlated with the current consumption of each SUT. The analysis of the total current consumption has revealed the imprecision of the FM assignment; as a

consequence, the original classification of system failures was modified and augmented. In the updated classification, the volume of errors identified as soft losses of functionality has been substantially increased.

The observed abrupt changes in SUT total current consumption turned out to be associated exclusively with the soft or hard losses of functionality; in both cases, the SUT recovery was required. System diagnostics based solely on the software observations resulted in disregarding multiple situations in which the SUT was in fact losing its functionality. The proposed observation technique can be thus used during the system-level test as an additional source of information used for determining the SUT condition.

The study case has demonstrated that the initial assumptions about the criticality of the observed failures can be erroneous; without the proposed observation method this would be, in the best case, revealed during the data postprocessing, or otherwise lead to the wrong conclusions about the system SEE sensitivity. However, the current consumption information can be used to reassess the classification of system failures during the performed test or in the posttest analysis, therefore improving its quality.

As an SUT diagnostics technique during system-level testing, the total current consumption monitoring should be executed in parallel with the normal data exchange with the SUT (through the digital or analog interface). Any abrupt change in the drawn current will be a probable consequence of the loss of functionality. The intervention will be then needed to verify by any possible means whether the SUT is still delivering its full functionality. Based on this, the conclusion can be made whether the SUT has encountered a FM that is transparent to it, or has suffered from the loss of functionality, and thus needs to be reconfigured or power-cycled. A set of software-level observations is advised to be implemented for the purposes of detailed system diagnostics after the encounter of the abrupt current change.

The described method will be included in the guidelines for system-level testing of accelerator electronics, however, this approach may be generalized and find applications elsewhere.

REFERENCES

[1] R. Ferraro, S. Danzeca, L. Dilillo, M. Brugger, A. Masi, and S. Gilardoni, "Estimation of system survival reliability in a radiation environment based on the available radiation data at component level," in *Proc. 17th Eur. Conf. Radiat. Effects Compon. Syst. (RADECS)*, Oct. 2017, pp. 1–8.

[2] S. Uznanski, R. G. Alía, M. Brugger, P. Moreira, and B. Todd, "Qualification of electronic components for a radiation environment: When standards do not exist," in *Proc. RADECS Short Course, 4B*, Geneva, Switzerland, 2017, pp. 1–55.

[3] R. G. Alia et al., "LHC and HL-LHC: Present and future radiation environment in the high-luminosity collision points and RHA implications," *IEEE Trans. Nucl. Sci.*, vol. 65, no. 1, pp. 448–456, Jan. 2018.

[4] S. Uznanski, B. Todd, A. Dinius, Q. King, and M. Brugger, "Radiation hardness assurance methodology of radiation tolerant power converter controls for large hadron collider," *IEEE Trans. Nucl. Sci.*, vol. 61, no. 6, pp. 3694–3700, Dec. 2014.

[5] C. Cazzaniga, M. Bagatin, S. Gerardin, A. Costantino, and C. D. Frost, "First tests of a new facility for device-level, board-level and system-level neutron irradiation of microelectronics," *IEEE Trans. Emerg. Topics Comput.*, vol. 9, no. 1, pp. 104–108, Jan. 2021.

[6] I. C. Lopes, V. Pouget, F. Wrobel, F. Saigne, A. Touboul, and K. Røed, "Development and evaluation of a flexible instrumentation layer for system-level testing of radiation effects," in *Proc. IEEE Latin-Amer. Test Symp. (LATS)*, Mar. 2020, pp. 1–6.

[7] J. Budroweit, S. Mueller, M. Jaksch, R. G. Alía, A. Coronetti, and A. Koelpin, "In-situ testing of a multi-band software-defined radio platform in a mixed-field irradiation environment," *Aerospace*, vol. 6, no. 10, p. 106, Sep. 2019.

[8] T. Rajkowski et al., "Comparison of the total ionizing dose sensitivity of a system in package point of load converter using both component- and system-level test approaches," *Electronics*, vol. 10, no. 11, p. 1235, May 2021.

[9] T. Rajkowski et al., "Analysis of SET propagation in a system in package point of load converter," *IEEE Trans. Nucl. Sci.*, vol. 67, no. 7, pp. 1494–1502, Jul. 2020.

[10] M. Rousselet, P. C. Adell, D. J. Sheldon, J. Boch, H. Schone, and F. Saigné, "Use and benefits of COTS board level testing for radiation hardness assurance," in *Proc. 16th Eur. Conf. Radiat. Effects Compon. Syst. (RADECS)*, Sep. 2016, pp. 1–5.

[11] R. Secondo et al., "System level radiation characterization of a 1U CubeSat based on CERN radiation monitoring technology," *IEEE Trans. Nucl. Sci.*, vol. 65, no. 8, pp. 1694–1699, Aug. 2018.

[12] K. Kruckmeyer, R. Eddy, A. Szczapa, B. Brown, and T. Santiago, "SEE testing of national semiconductor's LM98640QML system on a chip for focal plane arrays and other imaging systems," in *Proc. IEEE Radiat. Effects Data Workshop*, Jul. 2010, p. 8.

[13] M. Von Thun, Y. Lotfi, T. Meade, and A. Turnbull, "Single event latch-up and total ionizing dose characterization of a cobham designed smart power switch controller," in *Proc. IEEE Radiat. Effects Data Workshop (Conjunct With NSREC)*, Nov. 2020, pp. 1–5.

[14] C. Underwood, M. Unwin, R. H. Sorensen, A. Frydland, and P. Jameson, "Radiation testing campaign for a new miniaturised space GPS receiver," in *Proc. IEEE Radiat. Effects Data Workshop*, Jul. 2004, pp. 120–124.

[15] Y. Li et al., "Experimental study of transient dose rate effect on system-in-package SZ0501," *IEEE Trans. Nucl. Sci.*, vol. 69, no. 8, pp. 1840–1849, Aug. 2022.

[16] D. Prelipcean et al., "Benchmark between measured and simulated radiation level data at the mixed-field CHARM facility at CERN," *IEEE Trans. Nucl. Sci.*, vol. 69, no. 7, pp. 1557–1564, Jul. 2022.

[17] N. Trikoupis, J. Casas-Cubillos, and S. Danzeca, "Irradiation test results on cryogenics electronic cards using the Smartfusion2 FPGA," in *Proc. 18th Eur. Conf. Radiat. Effects Compon. Syst. (RADECS)*, Sep. 2018, pp. 1–6.

[18] A. de Bibikoff and P. Lamberbourg, "Method for system-level testing of COTS electronic board under high-energy heavy ions," *IEEE Trans. Nucl. Sci.*, vol. 67, no. 10, pp. 2179–2187, Oct. 2020.

[19] A. Coronetti et al., "Radiation hardness assurance through system-level testing: Risk acceptance, facility requirements, test methodology, and data exploitation," *IEEE Trans. Nucl. Sci.*, vol. 68, no. 5, pp. 958–969, May 2021.

[20] M. Cecchetto et al., "SEE flux and spectral hardness calibration of neutron spallation and mixed-field facilities," *IEEE Trans. Nucl. Sci.*, vol. 66, no. 7, pp. 1532–1540, Jul. 2019.

[21] A. Coronetti et al., "Thermal-to-high-energy neutron SEU characterization of commercial SRAMs," in *Proc. IEEE Radiat. Effects Data Workshop Rec.*, Jul. 2021, pp. 32–36.

[22] H. Quinn, "Challenges in testing complex systems," *IEEE Trans. Nucl. Sci.*, vol. 61, no. 2, pp. 766–786, Apr. 2014.

[23] D. M. Newberry, "Investigation of single event effects at the system level," in *Proc. 2nd Eur. Conf. Radiat. its Effects Compon. Syst. (RADECS)*, Sep. 1993, pp. 113–120.

[24] H. Rufenacht, D. M. Hiemstra, R. Ronge, T. Klincsek, K. A. Le, and J. Gazdewich, "Single event upset characterization of the ESP603 single board space computer with the PowerPC603r processor using proton irradiation," in *Proc. IEEE Radiat. Effects Data Workshop*, Jul. 2005, pp. 65–69.